NASA Technical Memorandum 101322
AIAA-88-3155

Vibration, Performance, Flutter and Forced Response Characteristics of a Large-Scale Propfan and Its Aeroelastic Model

Richard August
Sverdrup Technology, Inc.
NASA Lewis Research Center Group
Cleveland, Ohio

and

Krishna Rao V. Kaza
National Aeronautics and Space Administration
Lewis Research Center
Cleveland, Ohio

Prepared for the
24th Joint Propulsion Conference
cosponsored by the AIAA, ASME, SAE, and ASEE
Boston, Massachusetts, July 11-13, 1988

VIBRATION, PERFORMANCE, FLUTTER AND FORCED RESPONSE CHARACTERISTICS OF A LARGE-SCALE PROPFAN AND ITS AEROELASTIC MODEL

Richard August
Sverdrup Technology, Inc.
NASA Lewis Research Center Group
Cleveland, Ohio 44135

and

Krishna Rao V. Kaza
National Aeronautics and Space Administration
Lewis Research Center
Cleveland, Ohio 44135

ABSTRACT

An investigation of the vibration, performance, flutter, and forced response of the large-scale propfan, SR7L, and its aeroelastic model, SR7A, has been performed by applying available structural and aeroelastic analytical codes and then correlating measured and calculated results. Finite element models of the blades were used to obtain modal frequencies, displacements, stresses and strains. These values were then used in conjunction with a three-dimensional, unsteady, lifting surface aerodynamic theory for the subsequent aeroelastic analyses of the blades. The agreement between measured and calculated frequencies and mode shapes for both models is very good. Calculated power coefficients correlate well with those measured for low advance ratios. Flutter results show that both propfans are stable at their respective design points. There is also good agreement between calculated and measured blade vibratory strains due to excitation resulting from yawed flow for the SR7A propfan. The similarity of structural and aeroelastic results show that the SR7A propfan properly simulates the SR7L characteristics.

INTRODUCTION

One of the major research and technology programs at NASA Lewis Research Center is the advanced turboprop program (ATP). The goal of this effort is the development of turboprop (also known as propfan) propulsion systems which would have significant gains in fuel economy over turbofans without sacrificing aircraft performance (ref. 1). An important phase of this program is the large-scale advanced prop-fan program (LAP). This program is a joint effort between NASA and Hamilton Standard, and involves the development and fabrication of a complete eight-bladed, 2.743 m (9 ft) diameter propfan rotor (SR7L). The SR7L propfan that is being used in the LAP program is designed for a cruise Mach number of 0.80 at an altitude of 10.66 km (35 000 ft), with a rotational speed of 1700 rpm (fig. 1). In support of the flight test program for the SR7L, a scaled 2/9 model (SR7A) of the propfan was built prior to the actual construction of the SR7L propfan. The model is 62 23 cm (24.5 in.) in diameter and was designed to have the same structural dynamic and aeroelastic characteristics as the SR7L propfan. The SR7A propfan has been tested in the NASA Lewis Research Center (LeRC) 8x6-foot wind tunnel (fig. 2). Testing of the SR7L propfan is

being conducted through the Propfan Test Assessment (PTA) program, which is responsible for both ground and flight testing of the large-scale propfan.

The unique design features used to improve propeller performance have required new techniques and codes for the analysis of bladed propfan assemblies. The thin, twisted and highly swept, composite material blades experience large deflections due to blade flexibility, and centrifugal and aerodynamic loads. These blades operate in subsonic, transonic, and supersonic flows. Three-dimensional, steady and unsteady aerodynamics are necessary for the aeroelastic analysis of propfan blades with moderately small aspect ratios, and significant cascade effects.

In support of the ATP, research efforts at LeRC have addressed these features in order to improve structural modeling and aeroelastic analysis of propfans. Without listing a complete literature review, some areas where new analytical techniques have been recently implemented include modeling of blades constructed with composite materials (ref. 2), and geometric nonlinear analysis of flexible rotating blades based on plate theory (refs. 3 to 5). A three-dimensional, steady and unsteady aerodynamic theory for propfans with subsonic leading edge was formulated in reference 6. The theory was incorporated into the modal flutter code described in reference 7 for aeroelastic stability studies. This code has been further enhanced in reference 8 to calculate forced response due to yawed, or off-axis, flow. A stability analysis of SR7L using the above techniques was presented in reference 9.

The primary objective of this paper is the continued validation of these new analysis methods by applying the structural and aeroelastic codes to correlate theoretical and experimental results for the SR7A and SR7L propfans. This includes validating the codes for each propfan through comparison of frequencies and mode shapes, aeroelastic performance, flutter, and yawed flow forced response with available test data. A secondary objective is the assessment of the SR7A and SR7L dynamic simulation. This is accomplished by the direct comparison of analogous characteristics.

ANALYSIS METHODS

The procedure used to accomplish the objectives outlined above is schematically shown in figure 3. The first two steps calculate displacements and vibrational characteristics utilizing the finite element code, MSC/NASTRAN. The modal information is then used in conjunction with the aeroelastic code ASTROP (Aeroelastic STability and Response of Propulsion Systems) to calculate performance, flutter, and forced response.

Since aeroelastic analyses are sensitive to blade frequencies and mode shapes, it is important that the blade's finite element model and analysis accurately reflect its modal characteristics. By assuming a rigid hub, the blades are structurally decoupled from one another. Consequently, it is sufficient to structurally model just one blade. The modal analysis of advanced turboprop blades is complicated by the fact that these swept, twisted, and flexible blades have relatively large and nonlinear steady deflections due to centrifugal forces. It should be noted that the Coriolis forces have not been included in the normal modes analysis since they have been found to be negligible for thin, rotating blades (ref. 7). However, centrifugal softening effects are included in the analysis.

MSC/NASTRAN was used to calculate frequencies and modes shapes because it has the capability to perform geometric nonlinear analysis, as well as the capability to update the displacement dependent centrifugal forces. MSC/NASTRAN Solution 64 was used for the geometric nonlinear analysis. This solver uses a modified Newton-Raphson algorithm, along with load updating, to simulate the correct displacement versus load relationship. The algorithm iterations are controlled through "subcases," with a minimum of two being required. The first subcase computes the initial, linear deflected shape. Subsequent subcases, or iterations, then use the previously deflected shape to compute the differential stiffness matrix along with the new set of displacements. MSC/NASTRAN Solution 63 extracts the modal properties required for the aeroelastic analysis from the final mass and stiffness matrices that correspond to the blade's centrifugally deformed position.

The NASTRAN finite element models used in this study are based on the final blade designs (refs. 10 and 11). The SR7L blade has an aluminum spar and fiberglass shell with foam fill. The SR7A model has a shortened, titanium spar with a graphite reinforced fiberglass shell. Composite material properties were calculated by a micro-mechanics approach using available fiber and matrix properties obtained from material testing. Shell, adhesive, spar, and shell filler material were combined using the COmposite Blade STRuctural ANalysis (COBSTRAN) program to produce equivalent, monolithic shell elements (refs. 2 and 12).

The finite element models of the SR7A and SR7L blades are shown in figures 4(a) and (b), respectively. The SR7A model has 256 nodes and 449 triangular shell elements; the SR7L model has 261 nodes and 449 triangular shell elements. Bar elements are used to model the shank in both cases. Multipoint constraint cards that couple the displacement of prescribed grid points are used to define the shank/blade interface.

As mentioned previously, the structural analyses provide blade frequencies and mode shapes that are input for the aeroelastic analysis. The modal aeroelasticity code, ASTROP, is used to calculate the propfan performance, stability, and forced response. The analyses for both the SR7A and SR7L propfans use an eight-bladed propfan configuration consisting of identical blades, i.e., a tuned rotor.

The propfan steady performance is based on the blade pressure distribution, air density, rotor frequency, tip radius, and freestream velocity. Details on the nondimensionalization of the performance parameters are given in reference 13.

The aeroelastic stability is determined by solving the complex eigenvalue problem resulting from the propfan's homogeneous, aeroelastic equations of motion developed in reference 7. These equations are solved, with the vibratory motion expressed in terms of generalized coordinates based on the normal modes. Propfan damping and damped frequency are represented by the real and imaginary parts of the complex eigenvalue, respectively. Flutter occurs when the real part of the eigenvalue is greater than zero. The damping ratio can be calculated by dividing the real part of the eigenvalue by the magnitude of the complex eigenvalue.

The forced aeroelastic response of the propfan blade due to off-axis flow is an extension of the aeroelastic stability problem. Motion dependent aerodynamic forces at the reduced frequency corresponding to the rotational frequency of the rotor are included in the equations governing the response. Motion independent aerodynamic forces are used as forcing functions. These forces are based on a one-per-rev excitation due to a flow field inclined with respect to the axis of rotation. The forced response is calculated in terms of the generalized coordinates associated with the blade's normal modes and can be output as vibratory displacements, strains, or stresses.

RESULTS AND DISCUSSION

The structural dynamic and aeroelastic codes described above were used to analyze the SR7A and SR7L propfans. The results for the propfans are presented in following order: (1) comparison of the blades' mode shapes at an equivalently scaled rotational speed; (2) comparison of measured and calculated blade frequencies over a range of rotational speeds; (3) comparison of measured and calculated aerodynamic steady performance; (4) comparison of the propfans' damping plots and cascade effects on stability; and (5) comparison of SR7A's measured and calculated forced aeroelastic response.

Frequencies and Mode Shapes

To establish the validity of the finite element blade models, the calculated frequencies were compared with experimental values. Frequencies and corresponding mode shapes were calculated over a range of speeds and compared with those presented in references 10 and 11. Note that the calculated frequencies do not include the effect of steady airloads.

Figures 5(a) and (b) show the first four calculated mode shapes for the SR7A and SR7L blades, respectively. The mode shapes are at the SR7L design speed (1698 rpm) and the equivalently scaled SR7A rotational speed (7484 rpm). Both blades are at a 3/4 blade radius setting angle of 58°. The contour lines shown are based on relative displacements normal to the plane of rotation. Figures 6(a) and (b) show the modal displacements at the 3/4 blade chord, as viewed down the blade span.

The blades exhibit very similar mode shapes. The first mode is predominantly a first bending mode with fairly evenly spaced contours in the upper half of the blade. The spanwise view shows the motion to be primarily normal to the blade. The second mode is predominantly a first edgewise bending mode, with most of the motion occurring near the tip in the chordwise direction. The third mode can be classified as the second bending mode, since there is a generally chordwise nodal line near the tip. The fourth mode can be classified as the first torsional mode since there is a midchord nodal line. The fourth mode shows the greatest difference between the two blades, with the SR7A nodal line aft of the SR7L's.

Figures 7 and 8 show the comparison of the measured and calculated frequencies for both blades over a range of rotational speeds. For the SR7A blade, there is generally good agreement at the scaled design speed (7484 rpm)

and wind tunnel test speed (8400 rpm). The calculated fourth mode (first torsion) is softer, but within acceptable limits (<10 percent). The SR7L finite element model shows good agreement at the first, third, and fourth modes at the design speed (1698 rpm). The calculated second mode is much stiffer. However, since this is the edgewise mode, it will not have much influence on the aerodynamic forces. Also, this mode is the most sensitive to the support stiffness used in the finite element model, and therefore very difficult to model accurately (ref. 9).

Figure 9 shows a modified Campbell diagram to give a comparison of the two blades' calculated frequencies. Since the rotational speed ratios are inversely proportional to the blade diameter ratios, multiplying the frequencies by the tip radii would negate the size effects (ref. 10). The SR7A blade scaled frequencies are slightly higher than the SR7L blade scaled frequencies. However, the scaled frequencies are all within 10 percent of each other. Considering the complexities involved in modeling, designing, and constructing these composite blades, the agreement between the scaled frequencies is excellent.

Aerodynamic Steady Performance

Wind tunnel performance tests of the SR7A propfan were conducted in the NASA Lewis 8- by 6-ft Wind Tunnel (ref. 14). Figure 10 shows a comparison of the test results with the calculated SR7A performance. Both the analyses and the test were conducted at a constant freestream Mach number of 0.60, with the rotational speed varying from 7834 rpm (advance ratio $J = 2.5$) to 4897 rpm (advance ratio $J = 4.0$). The test blade's 3/4 span setting angle was measured to be 60.2° for a nonrotating condition. For comparison, the performance results were calculated based on undeformed, cold blade shapes.

The calculated results show generally good agreement with the test results, although the correlation with the experimental setting angle seems to worsen with increasing advance ratio. However, for the test conditions shown, the angle of the relative air velocity at the 3/4 blade radius chord, with respect to the blade, decreases as J increases from 2.5 to 4.0. Thus, it can be argued that the blade will untwist, i.e., setting angle decreases, as the advance ratio increases. Therefore, there is good agreement between calculated and measured results at lower blade setting angles with higher values of J.

A second study, using the SR7L blade, examined the effect of the blade's steady, deformed shape on the calculated performance. This was done because the performance values are very sensitive to the blade setting as demonstrated by the experimental results in reference 13. For the constant blade setting angle shown in figure 10, the calculations do not include the effects of centrifugal loads nor steady airloads on the blade's steady state configuration. Instead, changes to the blade setting angles were done through rigid body rotations about the blade span. A better approximation of the blade's deformed shape can be obtained by adding deflections due to both centrifugal and aerodynamic loads to the nonrotating blade geometry.

These deflections can be properly calculated by iterating on the process described in figure 3. Basically, a centrifugally displaced geometry is used to calculate steady aerodynamic pressures, which are then used to calculate a new deformed shape due to combined centrifugal and steady aero loads. The

process is repeated until a converged, deformed geometry is obtained. It should be noted that this procedure is computationally intensive, considering the CPU time and memory storage required.

Figure 11 shows how the SR7L's blade 3/4 radius setting angle changes and converges through four iterations, for two different advance ratios. The setting angles are shown normalized by their nonrotating, cold shape value. The effective Mach numbers at the blade tip are 0.97 and 0.87 for $J = 3.6$, and $J = 2.2$, respectively. Just the centrifugal effects can be seen in the first iteration. The amount of blade untwist is greater at $J = 2.2$ since the rotational speed is higher than that at $J = 3.6$. The remaining iterations show the effect of combined centrifugal and aerodynamic loads. Introducing the aerodynamic loads increases the blade twist. The aerodynamic effects are shown to be more significant for the higher advance ratio, primarily due to higher effective air velocity. In fact, the calculated aerodynamic loads are shown to completely offset the centrifugal untwist and increase the final blade setting angle.

Figure 12 shows the effect of the aeroelastic iterations on the calculated SR7L performance parameters. The purpose of the calculations was to converge to a given power coefficient based on a fully loaded blade, starting from a cold shape blade setting angle. The initial starting point was made on a trial and error basis. Comparisons were then made between calculated and measured thrust and power coefficients for three test cases (ref. 15). Results are shown, and labeled, for the calculated performance values corresponding to the iterations described in figure 11.

There was good agreement for the two test points at the lower advance ratio of $J = 2.2$. The general trend between experiment and calculation was very close, with the calculated values being offset slightly higher. For the higher value of J, the agreement was poor for the one available test point. However, the blade tip velocity was transonic, and the linear subsonic aero theory was probably not accurately predicting the aerodynamic loads.

Aeroelastic Stability Results

Figures 13 and 14 show the predicted aerodynamic damping (real part of the system eigenvalue) at the design rotational speeds as a function of freestream Mach number. The blades are shown to be stable at the design point of Mach 0.8 and at an altitude of 10.66 km (35 000 ft). To estimate the available flutter margin for the propfans, the analysis was extended to calculate aerodynamic damping for freestream Mach numbers greater than 0.8. The damping values shown are for the most unstable interblade phase angles. The figures show the propfans to be very aeroelastically similar in predicting the same instability point, as well as identifying the same unstable interblade phase angle for the specific mode analyzed.

Modes one and three are stable over the range of Mach numbers with only minimal differences between the two propfans in the calculated damping for mode one. The differences in the mode three damping can be attributed in part to the slight differences in the third mode shape. The SR7A has more tip motion, particulary at the trailing edge, due to the node line descending a little further down the blade. The SR7L's node line is mainly along a blade chord,

reducing the overall tip motion and consequently, reducing the aerodynamic loading and damping. Mode two shows consistently low damping values for both propfans since this is the first edgewise mode, and always has small aerodynamic loads.

The fourth mode becomes unstable at a freestream Mach number of 0.90, well above the design Mach number. The analysis also indicates very little mode coupling, which suggests single mode flutter. The severity and type of the instability at that point, however, are questionable. The strength and significance of transonic effects on propfan flutter are still being investigated for the regions at which the SR7L instability is predicted. It should be noted that the blade designer, Hamilton Standard, used a two-dimensional aerodynamic code and predicted a third mode instability with little mode coupling; and relatively high damping values for the fourth mode (ref. 11).

The damping values shown in the above figures are considered to be conservative, since neither material nor friction damping due to the hub constraint have been included in the analysis. Additional system damping would only have a stabilizing effect. From these results, it is concluded that the SR7L propfan is free from flutter at the design point.

Cascade Effects

To illustrate the effects of cascade aerodynamics on blade stability, parametric studies were made varying the number of blades in the SR7A propfan model. Figure 15 is an example of a root locus plot for the first mode. This figure shows the phase relationship between blades by plotting the imaginary part of the system eigenvalue, i.e., the damped natural frequency, against the real part of the eigenvalue, which is an indicator of the system stability. It demonstrates the de-stabilizing influence of the cascade effect, as the length of the semi-major axis of the ellipse increases with additional blades. Also note that the aeroelastic frequency is being reduced with increased blading. An indication of the robustness of the first mode stability is shown by the fact that the system remains stable even with increased blading. Although not shown, the fourth mode also displays the same trends by remaining stable with increasing blading. These results are consistent with the calculated cascade effects found on the SR7L propfan (ref. 9).

Forced Response Results

Recently, the ASTROP code was expanded to include the capability to perform forced vibration analysis of aerodynamically excited propfans. By yawing the propfan's axis of rotation with respect to the air flow, the blades' angle of attack change at a one per rev frequency, causing periodic aerodynamic loading on the blades. The capability to accurately predict these loads and blade response is critical to the successful design of propfans.

The SR7A propfan was tested at the NASA-Lewis 8x6 foot wind tunnel for one-per-rev (1P) response. One blade was strain-gaged to measure vibratory response due to the aerodynamic excitation. One test case from the report (ref. 16) describing the vibratory response tests was selected with which to

compare analytical predictions. A subsonic case was used since only a subsonic, forced response version of the code was available at the time of this study.

The test operating conditions were used as input for the ASTROP code. These include inflow angle, freestream velocity, air pressure, rotational speed, and blade setting angle. In addition, frequencies, mode shapes, and modal strains were recalculated at the test speed.

Table I shows the comparison between the measured and calculated 1P vibratory strains for three different strain measurement locations from the one test case. The range of strains from the analysis is the elemental vibratory strains in the immediate vicinity of the strain gage location. The analysis has generally good agreement for the mid-blade location, but predicts lower strain in the tip region. The degree of agreement of the analytical results is consistent with that presented in reference 8 for another composite blade, SR3CX2; and for the metallic blade, SR5. In those cases, better agreement between measured and calculated strains occur at the in-board location rather than at the tip. This demonstrates the difficulty in accurately modeling the tip motion and its effects on tip aerodynamic loading.

Another factor that affects the analytical predictions is the material modeling of the composite blade. Modeling of the composite material is done over a larger area, and will tend to average out the material property values. This is particulary important in the spar/graphite interface areas, such as the tip, where two dissimilar materials are modeled as one, averaged, monolithic element.

SUMMARY OF RESULTS

An investigation of the vibration and aeroelastic characteristics of the SR7A and SR7L propfans has been performed using finite element models of the propfan blades and a three-dimensional aeroelasticity code. Analytical results were compared with available measured data to validate the analysis. The results show that:

1. With the exception of the edgewise mode, there is generally good agreement between calculated and measured frequencies. The analytical mode shapes of the SR7A and SR7L blades are very similar. Scaling the natural frequencies by the tip radius show that the SR7A blade matches the dynamic characteristics of the SR7L blade very well.

2. The aerodynamic performance calculations show good agreement with the test results for two specific cases, and, in general, match the proportionality relationships between thrust and power coefficients for that operating condition. Performance results are quite sensitive to the blade setting angle.

3. The propfans are stable at their respective design points. They show similar damping values, as well as identical least stable interblade phase angles. Both predict flutter at a Mach number higher than the design Mach number.

4. Cascade effects are appreciable for the SR7A propfan, as for the SR7L propfan. Increasing the number of blades decreases the frequency of the lowest damped mode, and decreases the amount of system damping, although the system does remain stable at the design operating condition.

5. Forced response calculations for the SR7A propfan show better agreement at blade mid-span than at the tip; an observation consistent with analyses of other propfans.

6. Based on the good agreement between the analytical results for the SR7A and SR7L propfans, with respect to structural modal characteristics and aeroelastic behavior, the SR7A propfan properly simulates the SR7L behavior.

REFERENCES

1. Whitlow,J.B. JR. and Sievers, G.K.: "Fuel Savings Potential for the NASA Advanced Turboprop Program", NASA TM-83736, 1984.

2. Aiello, R.A. and Chi, S., "Advanced Composite Turboprops: Modeling, Structural and Dynamic Analyses," ASME Paper 87-GT-78, 1987.

3. NASTRAN Theoretical Manual, NASA SP-221(06), 1977.

4. Lawrence, C. and Kielb, R.E., "Nonlinear Displacement Analysis of Advanced Propeller Structures Using NASTRAN," NASA TM 82727, August 1984.

5. Lawrence, C., et. al., "A NASTRAN Primer for the Analysis of Rotating Flexible Blades," NASA TM 89861, May, 1987.

6. Williams, M.H. and Hwang,C., "Three-Dimensional Unsteady Aerodynamics and Aeroelastic Response of Advanced Turboprops," Presented at the AIAA 27th Structures, Structural Dynamics, and Materials Conference, Part 2, New York, 1986, pp.116-124.

7. Kaza, K.R.V., et. al., "Analytical Flutter Investigation of a Composite Propfan Model," AIAA Paper 87-0738, Presented at the AIAA/ASME/ASEE/AHS 28th Structures, Structural Dynamics, and Materials Conference, CA, April, 1987.

8. Kaza, K.R.V., et al: "Aeroelastic Response of Metallic and Composite Propfan Models in Yawed Flow", AIAA Paper 88-3154, Presented at the AIAA/ASEE/ASME/SAE 24th Joint Propulsion Conference and Exhibit, July 11-14, 1988, Boston, MA.

9. August, R. and Kaza, K.R.V., "Vibration and Flutter Characteristics of the SR7L Large-Scale Propfan," NASA TM 100272, January, 1988.

10. Nagle, Auyeung, Turnberg, "SR7A Aeroelastic Model Design Report," NASA CR 174791, October, 1986.

11. Sullivan, W.E., Turnberg, J.E., Violette, J.A., "Large-Scale Advanced Propfan (LAP) Blade Design," NASA CR 174790.

12. Chou, S. "SR7L Turboprop Blade Finite Element Model," Sverdrup Topical Report, March, 1986.

13. Williams, M.H., "Users's Guide to UPROP3S," Purdue University Report, June, 1985.

14. Stefko, G.L., et al: "Wind Tunnel Performance Results of an Aeroelastically Scaled 2/9 Model of the PTA Flight Test Prop-Fan", AIAA Paper No. 87-1893 (NASA TM 89917), July, 1987.

15. Campbell, W.A, Wainauski, H., and Bushnell, P.R., "A Report on High Speed Wind Tunnel Testing of the Large Scale Advanced Prop-Fan," AIAA Paper 88-2802, Presented at the AIAA/ASEE/ASME/SAE 24th Joint Propulsion Conference and Exhibit, July 11-14, 1988, Boston, MA.

16. Hamilton Standard Memo Report 267X-206, "Experimental and Analytic Evaluation of the SR7A Aeroelastic Model 1P Vibratory Response," August 19, 1986.

TABLE I. - COMPARISON OF MEASURED AND CALCULATED ONE PER REV VIBRATORY STRAIN

[Inflow angle = 2.08°; Tunnel Mach number = 0.6; rpm = 8004; Setting angle = 51.85°.]

Gage location	Blade radius, percent	Chord, percent	Test data[a]	Analysis range[a]
Mid-blade	70	59	138	70 to 130
Tip-bending	86	67	119	40 to 61
Tip shear	86	67	91	47 to 67

[a]Strain given in micro-in./in.

FIGURE 1. - SR7L PROPFAN FLIGHT TEST.

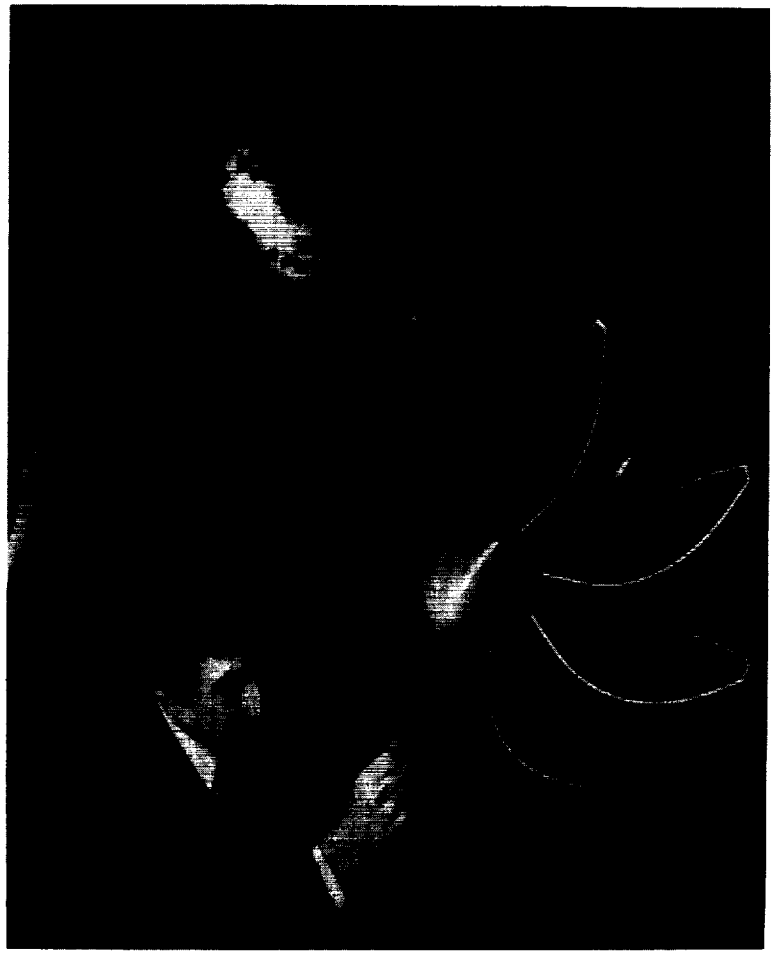

FIGURE 2. - SR7A PROPFAN WIND TUNNEL TEST CONFIGURATION.

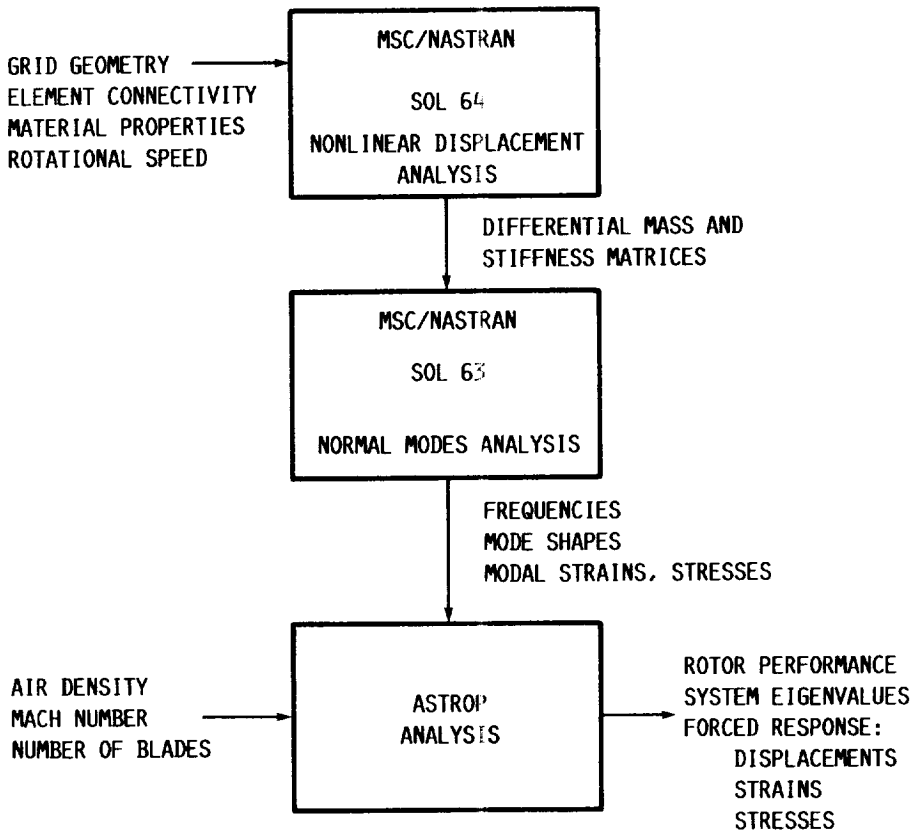

FIGURE 3. - PROPFAN ANALYSIS METHODOLOGY.

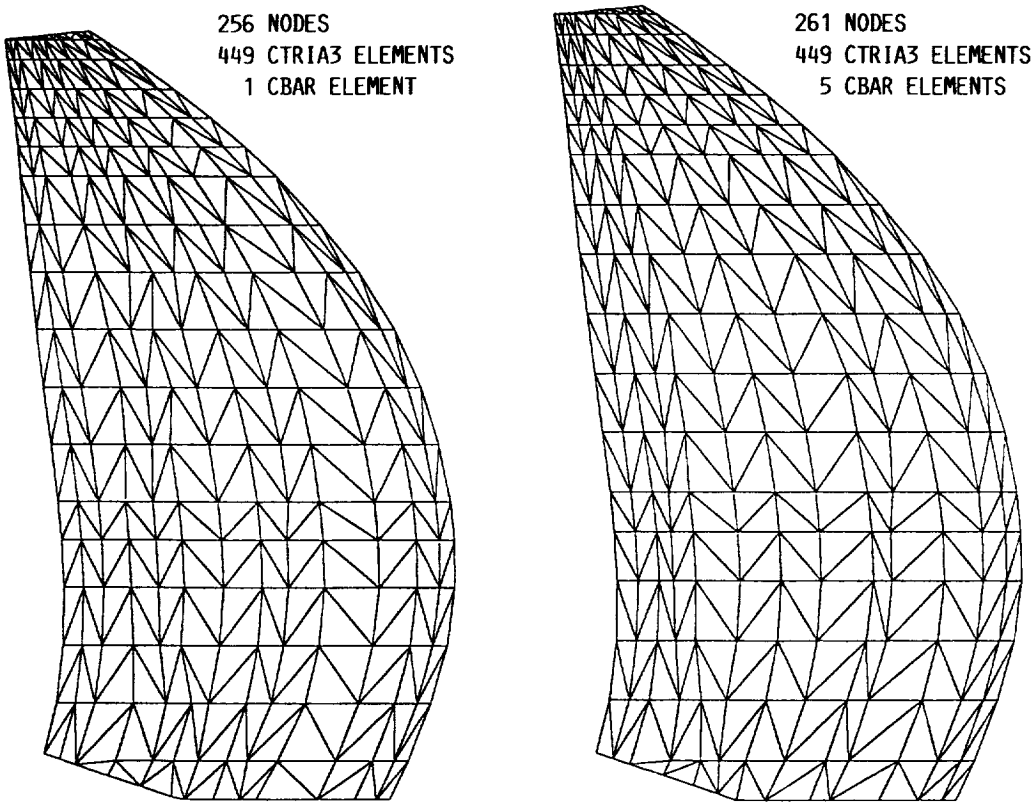

(A) SR7A (B) SR7L

FIGURE 4. - PROPFAN BLADE FINITE ELEMENT MODELS.

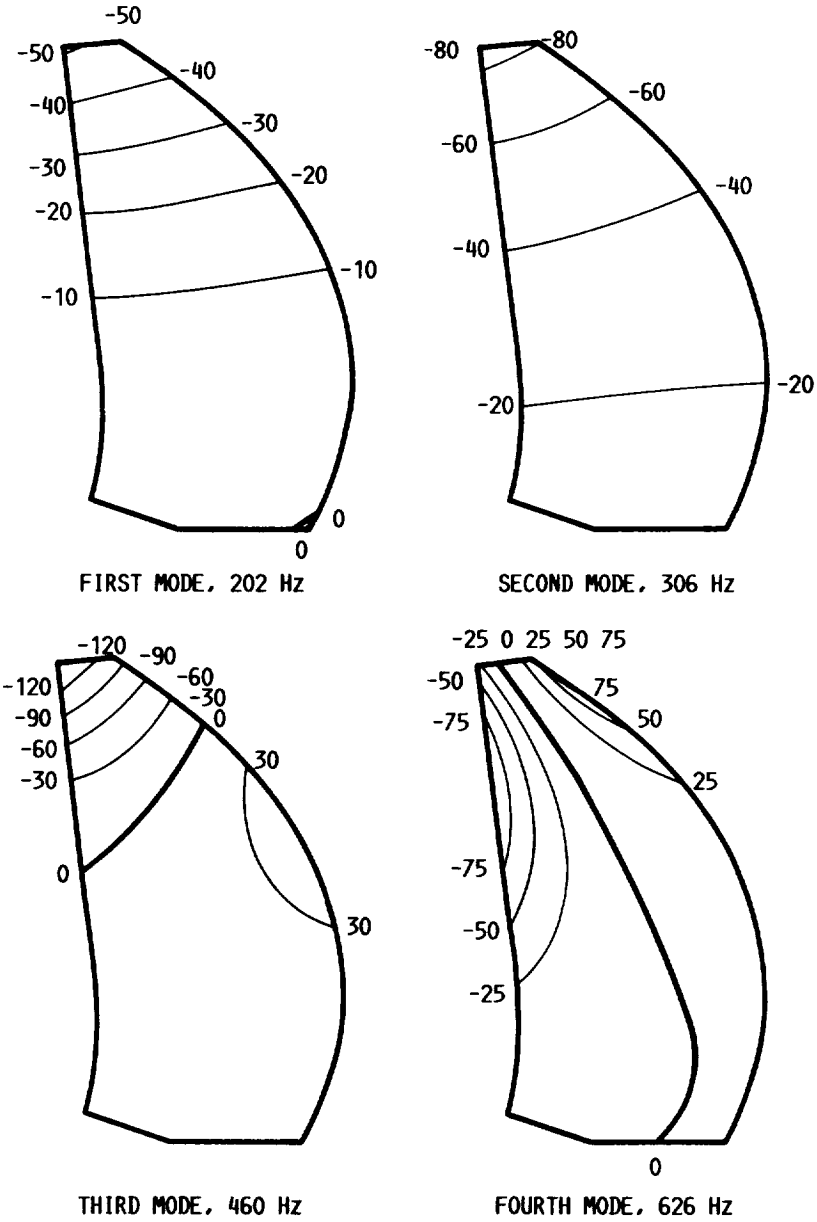

(A) SR7A, 7484 RPM.

FIGURE 5. - CALCULATED FREQUENCIES AND MODE SHAPES (CONTOUR LINES SHOW RELATIVE DISPLACEMENTS NORMAL TO PLANE OF ROTATION).

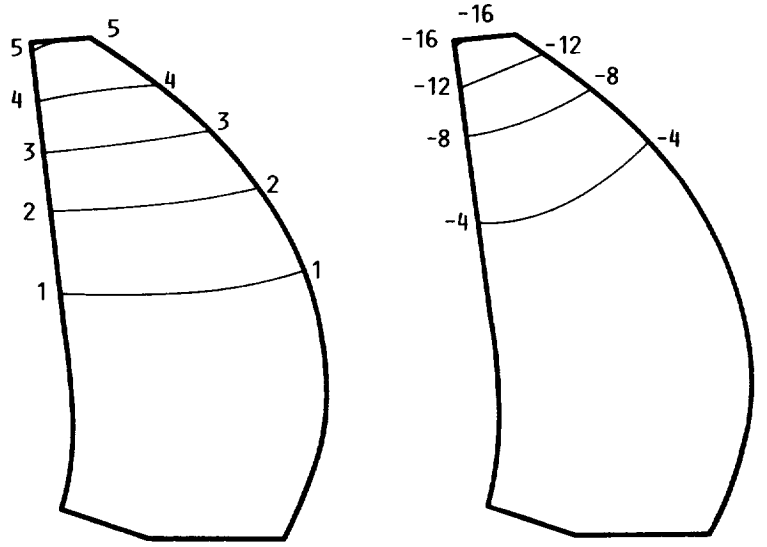

FIRST MODE, 43 Hz

SECOND MODE, 84 Hz

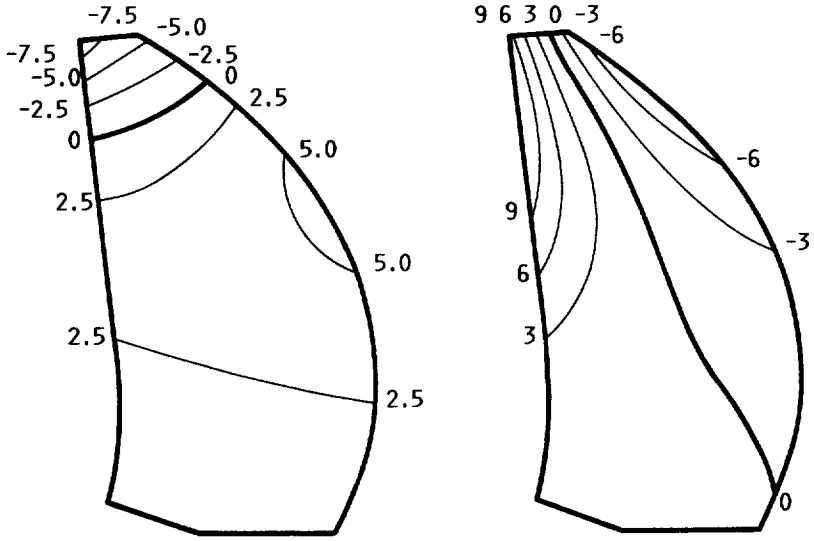

THIRD MODE, 107 Hz

FOURTH MODE, 143 Hz

(B) SR7L, 1698 RPM.

FIGURE 5. - CONCLUDED.

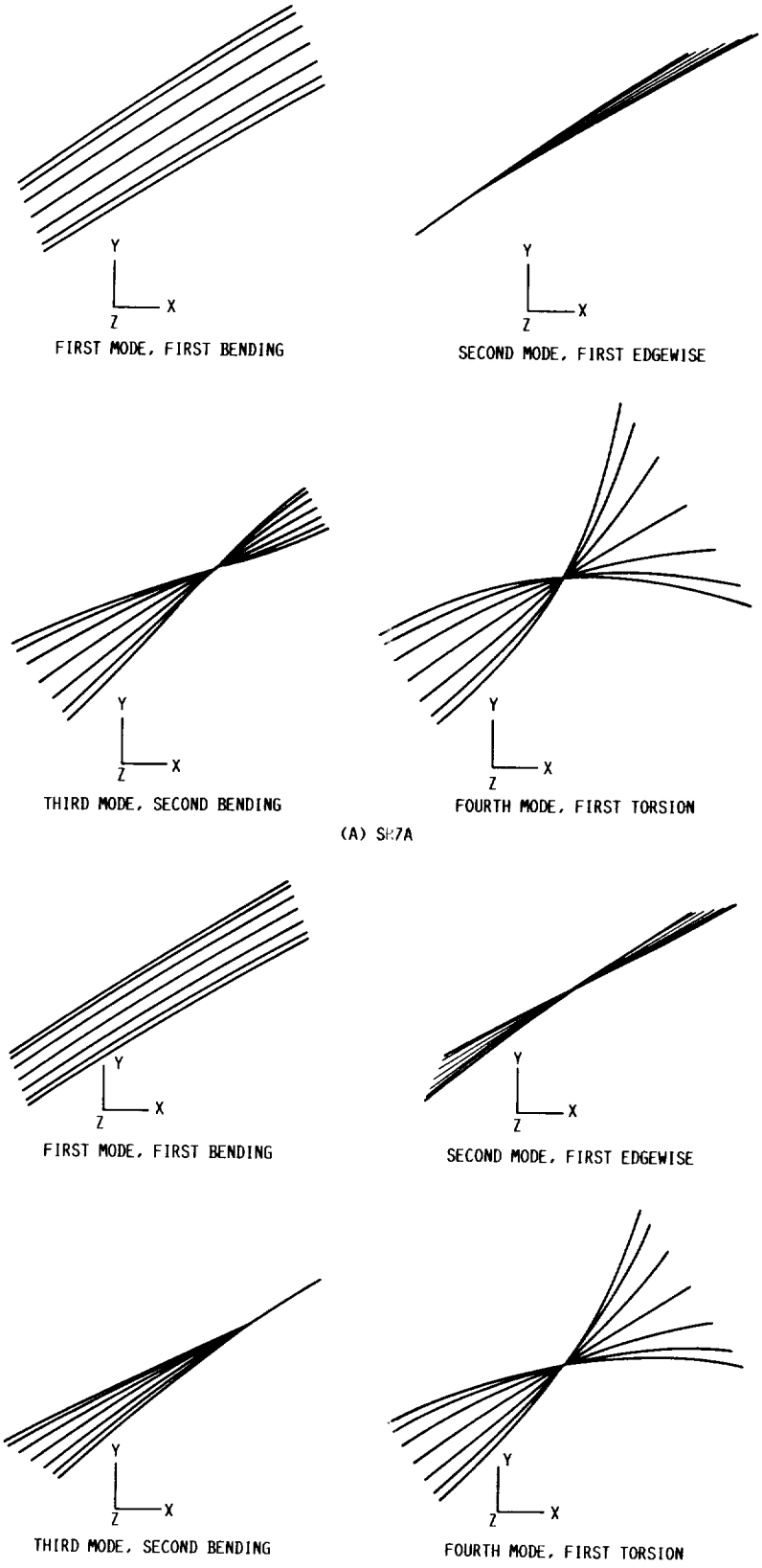

FIGURE 6. - MODAL DISPLACEMENT (SPAN-WISE VIEW) BLADE CHORD MODAL DISPLACEMENT AT 3/4 SPAN RADIUS.

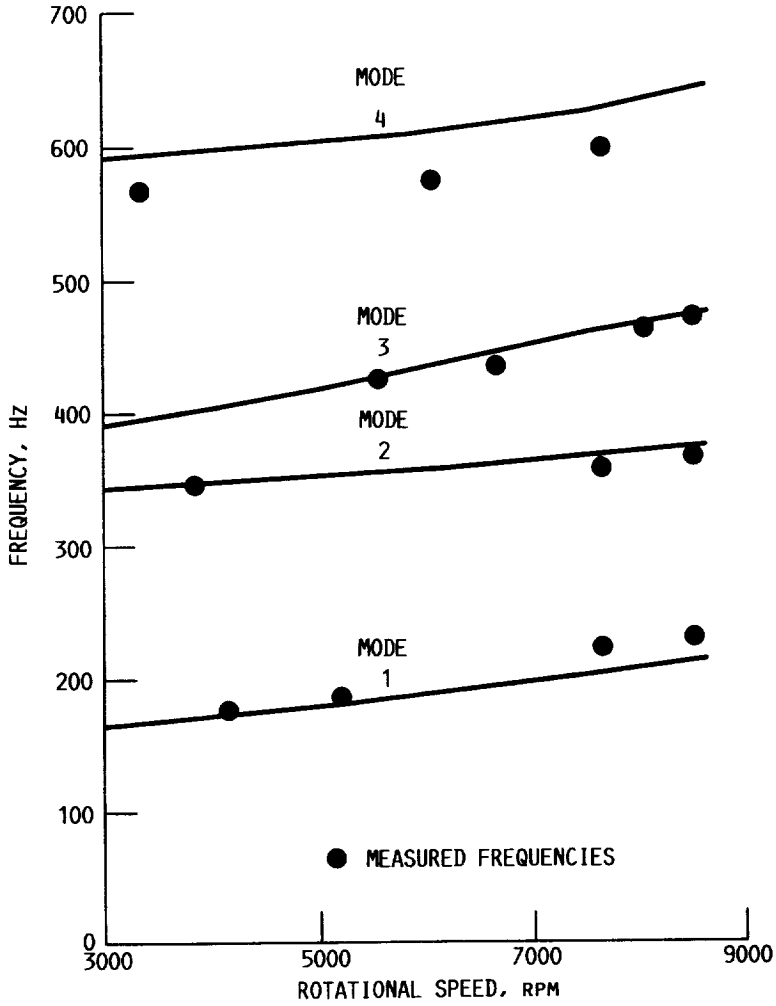

FIGURE 7. - CALCULATED SR7A FREQUENCIES VERSUS RPM.

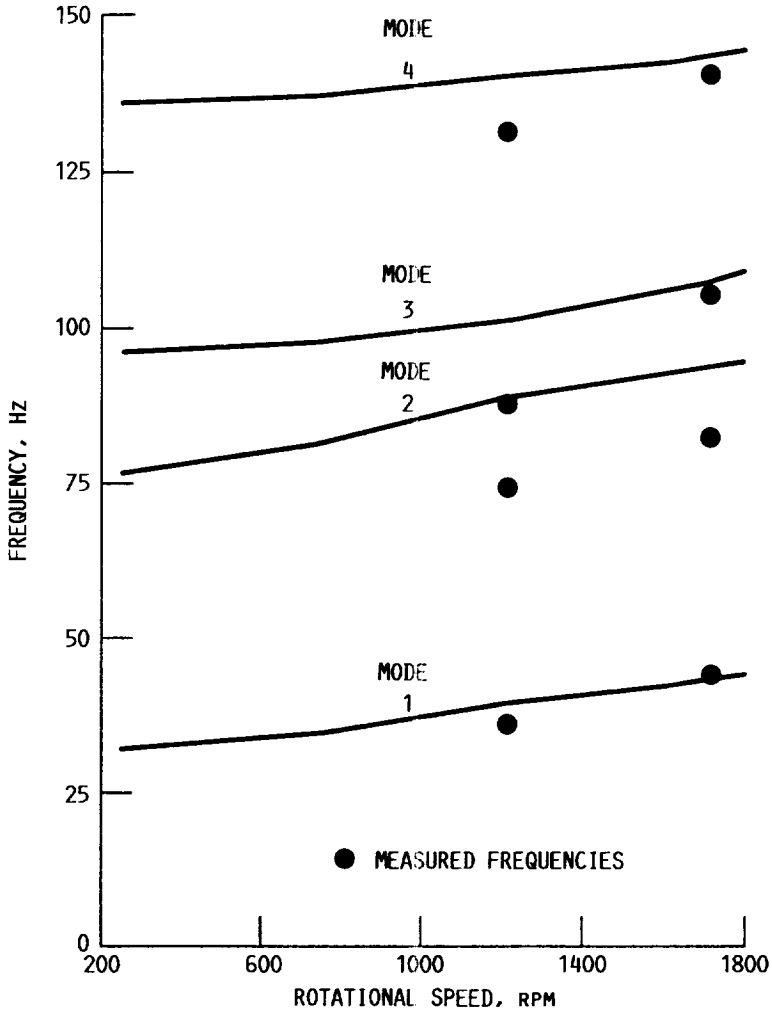

FIGURE 8. - CALCULATED SR7L FREQUENCIES VERSUS RPM.

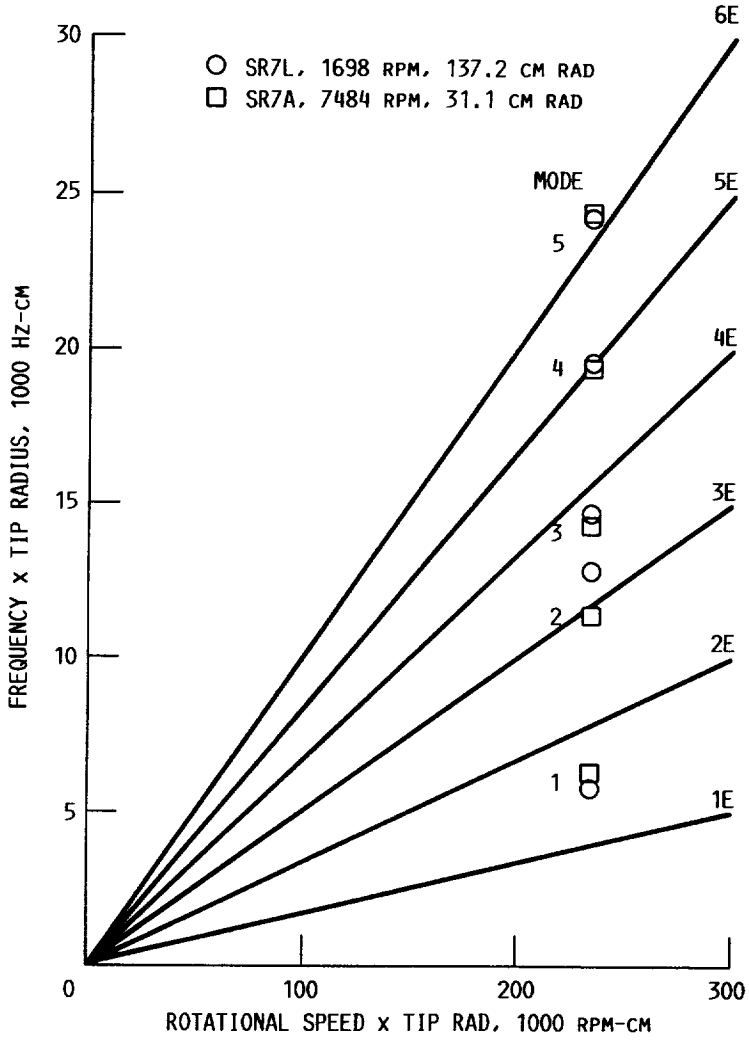

FIGURE 9. - SR7A, SR7L MODIFIED CAMPBELL DIAGRAM WITH CALCULATED FREQUENCIES.

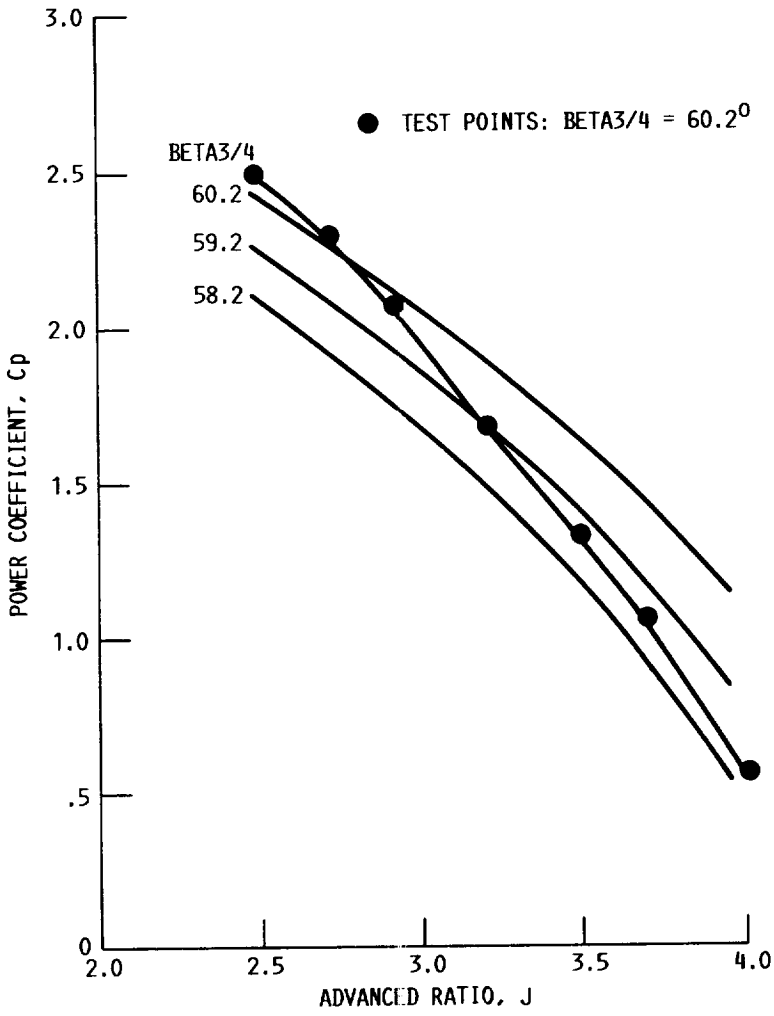

FIGURE 10. - SR7A CALCULATED POWER COEFFICIENTS VERSUS ADVANCE RATIO, MACH 0.6.

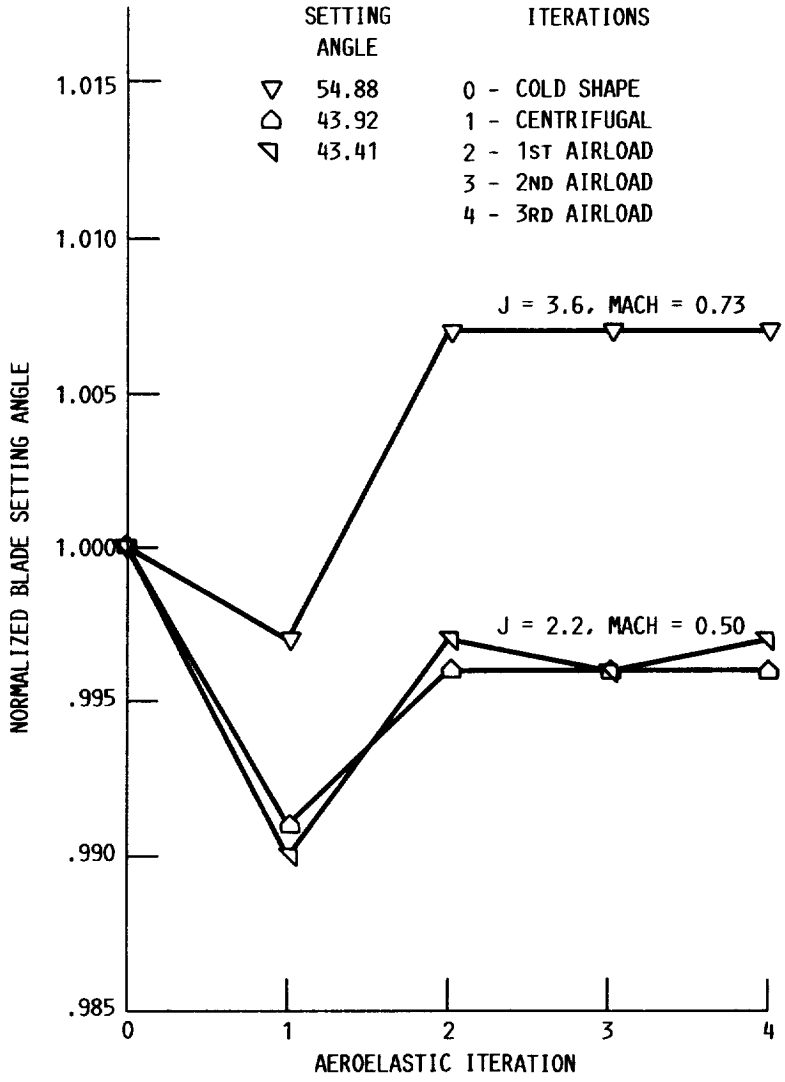

FIGURE 11. - NORMALIZED SR7L BLADE SETTING ANGLE VERSUS AEROELASTIC ITERATION.

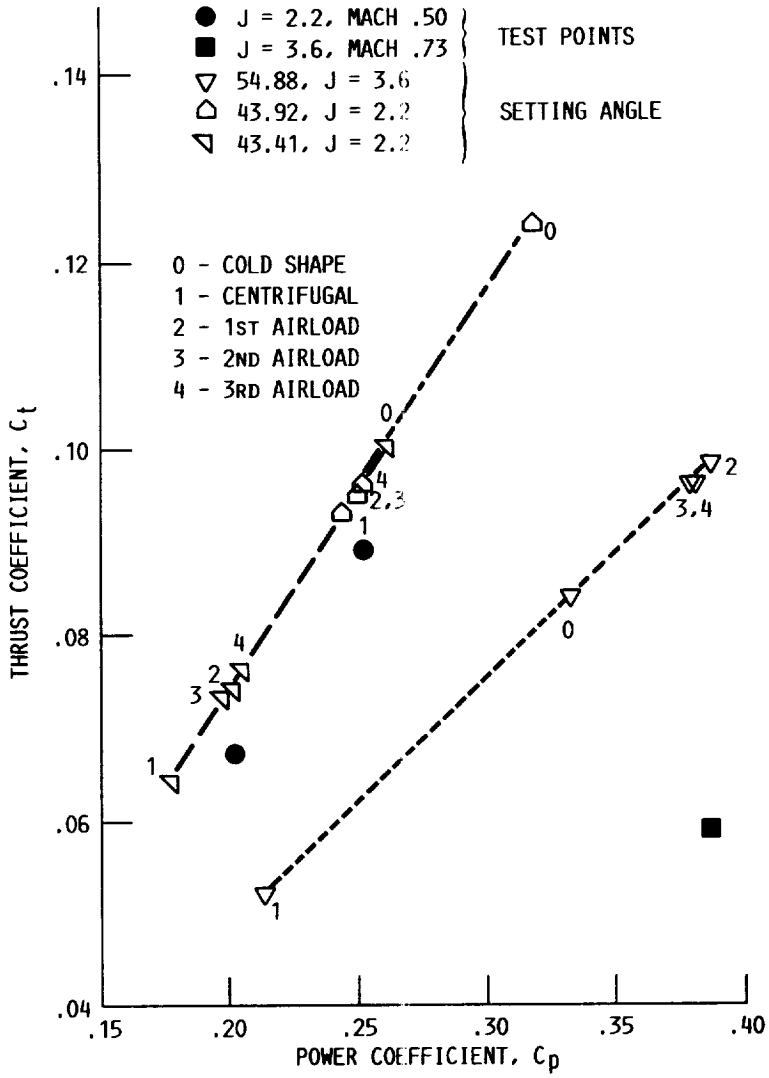

FIGURE 12. - SR7L CALCULATED THRUST COEFFICIENT VERSUS AEROELASTIC ITERATION.

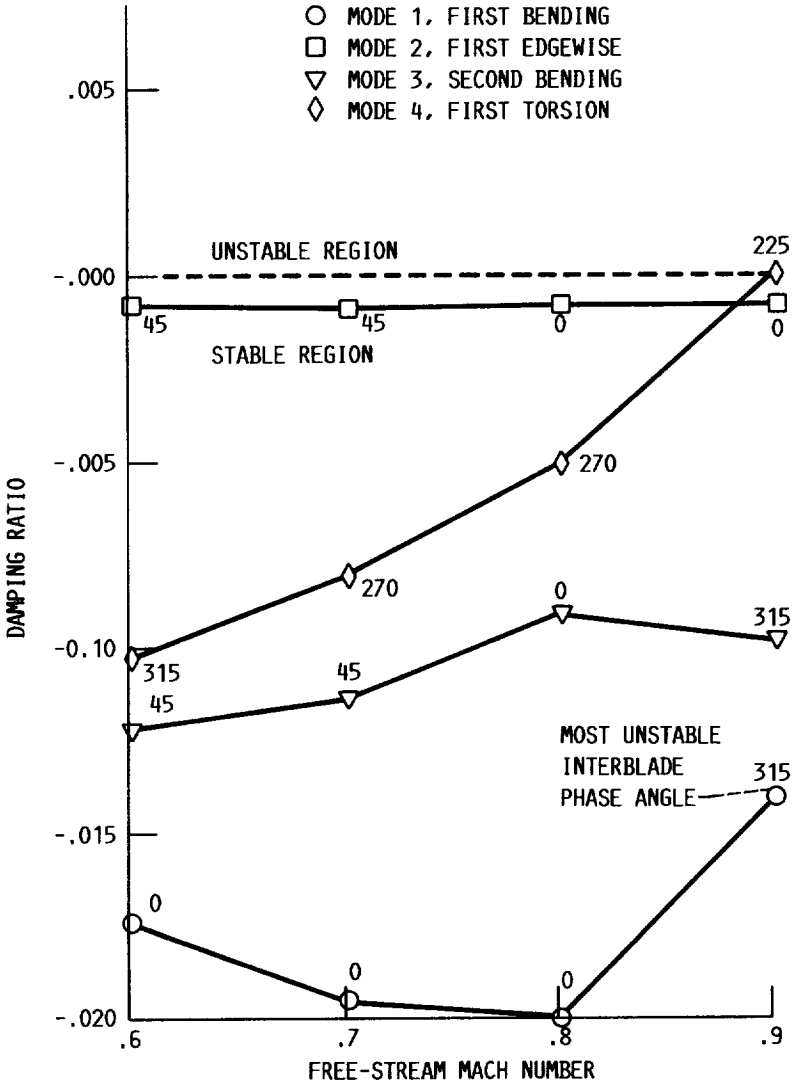

FIGURE 13. - SR7A CALCULATED DAMPING RATIO.

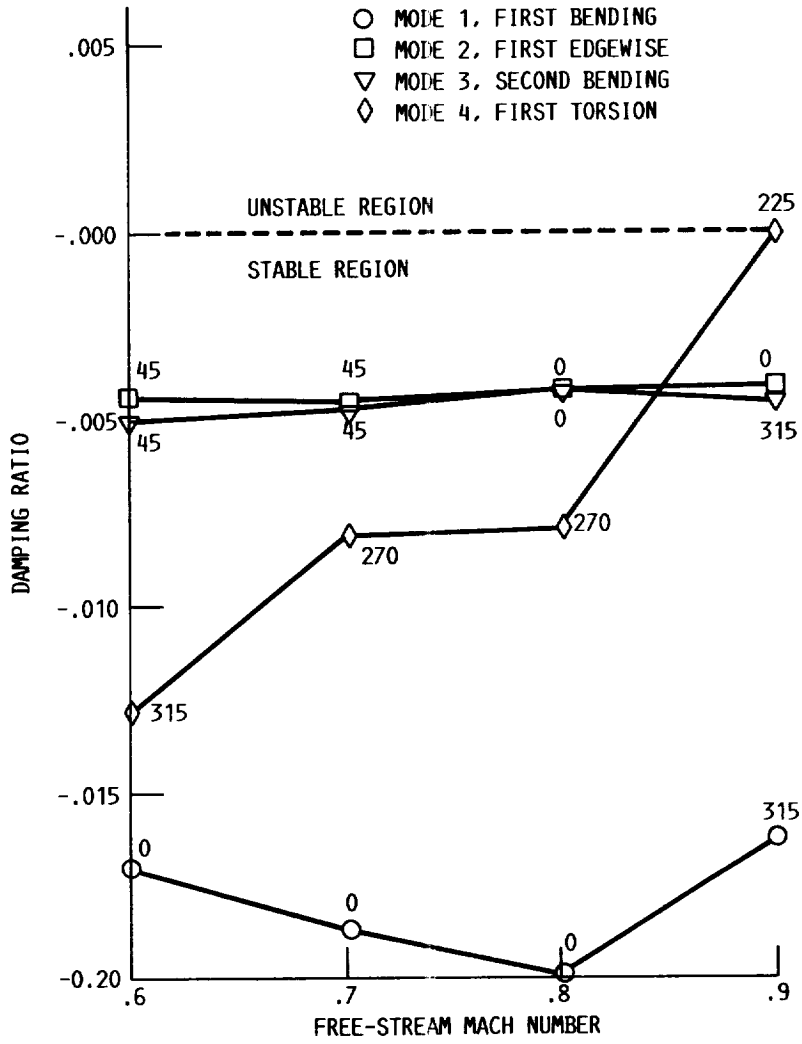

FIGURE 14. - SR7L CALCULATED DAMPING RATIO.

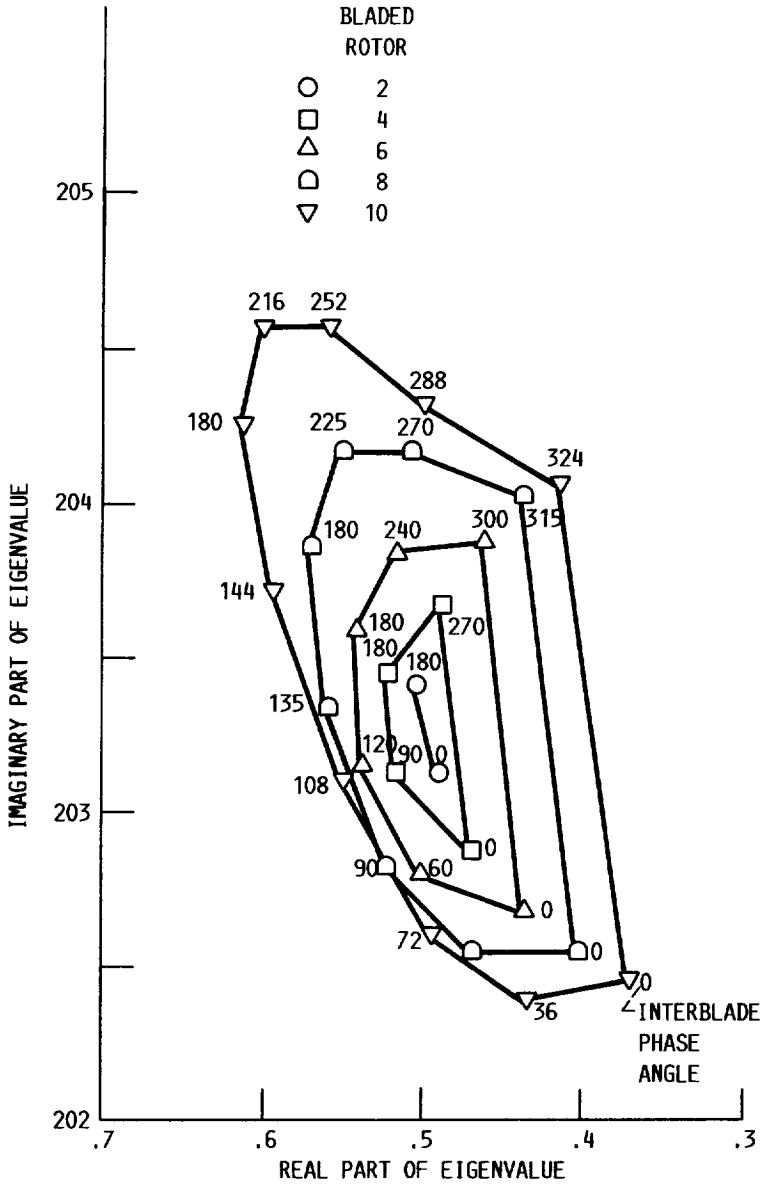

FIGURE 15. - SR7A CASCADE EFFECT ON MODE ONE ROOT LOCUS PLOT.

NASA
National Aeronautics and Space Administration

Report Documentation Page

1. Report No.	2. Government Accession No.	3. Recipient's Catalog No.
NASA TM-101322 AIAA-88-3155		

4. Title and Subtitle

Vibration, Performance, Flutter and Forced Response Characteristics of a Large-Scale Propfan and Its Aeroelastic Model

5. Report Date

6. Performing Organization Code

7. Author(s)

Richard August and Krishna Rao V. Kaza

8. Performing Organization Report No.
E-4260

10. Work Unit No.
505-63-1B

9. Performing Organization Name and Address

National Aeronautics and Space Administration
Lewis Research Center
Cleveland, Ohio 44135-3191

11. Contract or Grant No.

13. Type of Report and Period Covered
Technical Memorandum

12. Sponsoring Agency Name and Address

National Aeronautics and Space Administration
Washington, D.C. 20546-0001

14. Sponsoring Agency Code

15. Supplementary Notes

Presented at the 24th Joint Propulsion Conference cosponsored by the AIAA, ASME, SAE, and ASEE, Boston, Massachusetts, July 11-13, 1988. Richard August, Sverdrup Technology, Inc., NASA Lewis Research Center Group, Cleveland, Ohio 44135; Krishna Rao V. Kaza, NASA Lewis Research Center.

16. Abstract

An investigation of the vibration, performance, flutter, and forced response of the large-scale propfan, SR7L, and its aeroelastic model, SR7A, has been performed by applying available structural and aeroelastic analytical codes and then correlating measured and calculated results. Finite element models of the blades were used to obtain modal frequencies, displacements, stresses and strains. These values were then used in conjunction with a three-dimensional, unsteady, lifting surface aerodynamic theory for the subsequent aeroelastic analyses of the blades. The agreement between measured and calculated frequencies and mode shapes for both models is very good. Calculated power coefficients correlate well with those measured for low advance ratios. Flutter results show that both propfans are stable at their respective design points. There is also good agreement between calculated and measured blade vibratory strains due to excitation resulting from yawed flow for the SR7A propfan. The similarity of structural and aeroelastic results show that the SR7A propfan properly simulates the SR7L characteristics.

17. Key Words (Suggested by Author(s))	18. Distribution Statement
Mode shapes; Large scale propfan; Dynamic analysis; Blade flutter; Aeroelastic computer code; Rotor performance; Rotor forced response	Unclassified – Unlimited Subject Category 07

19. Security Classif. (of this report)	20. Security Classif. (of this page)	21. No of pages	22. Price*
Unclassified	Unclassified	28	A03

*For sale by the National Technical Information Service, Springfield, Virginia 22161